Second Harmonic Generation in Carbon Dioxide Processed Thin Polymer Films

Stephen E. Barry and David S. Soane*

Department of Chemical Engineering, The University of California at Berkeley, Berkeley, California 94720

Received February 13, 1996[⊗]

ABSTRACT: Polymer films were swelled with carbon dioxide (CO_2), allowing the alignment of second harmonic generating (SHG) chromophores with an electric field at ambient temperatures. SHG decay provided information on the glassy structure, the alteration of the glassy structure by a CO_2 sorption−desorption cycle, and molecular motion in a glassy polymer matrix. The host−guest system of poly(methyl methacrylate)−Disperse Red 1 was studied in most of the experiments; polycarbonate films were also examined. Chromophore alignment was less stable when either high CO_2 pressure or fast CO_2 desorption was used. After chromophore alignment, the films exhibited a multimodal decay of second harmonic generation capability. A fast decay was followed by a slow decay hypothesized to depend on the α-relaxation.

Introduction

Organic chromophores with large permanent electric dipoles separated by a delocalized π-bond structure have the largest known second-order hyperpolarizabilities of any class of materials.[1,2] Waveguides formed from polymer thin films in which the chromophores are incorporated can be used for second-order nonlinear optical applications such as second harmonic generation (SHG) and electrooptical modulators.[3,4] The chromophores can be dissolved in a host polymer, covalently bonded to the polymer as a side chain, or incorporated into the main chain of the polymer.

The alignment of the chromophore dipoles is necessary for bulk SHG.[5] Because the chromophores possess large permanent electric dipole moments, they may be aligned by applying a strong electric field.[6,7] When the interaction energy between the electric field and the dipole is small with respect to the prevailing thermal energy, the macroscopic hyperpolarizability χ has the approximate functionality[8]

$$\chi \propto N\beta\frac{\mu E}{kT} \tag{1}$$

where N is the chromophore number density, β is the molecular hyperpolarizability, μ is the chromophore dipole moment, and E is the applied dc electric field. Thus χ depends on the degree of alignment of the dipoles. The aligning energy of the field acting on the permanent dipole moment of the chromophore, μE, is opposed by the randomizing energy of Brownian motion, kT.

Chromophore alignment is expediently accomplished while the polymer is in a softened state. Typically, the polymer is softened by heating the polymer close to or above its glass transition. At this elevated temperature, the chromophores can be aligned with the applied dc electric field. Then the sample is cooled below the glass transition to room temperature, yielding a material with a relatively stable SHG signal. However, as seen in eq 1, poling at an elevated temperature causes a decrease in the chromophore orientational order, reducing the macroscopic second-order susceptibility. As the temperature needed to bring about the glass transition is increased, the strength of the electric field needed to obtain a given degree of chromophore alignment is increased. The maximum strength of the electric field that can be applied to orient the chromophore is limited by the dielectric breakdown strength of the material. Thus, for polymers with high T_g's, poling above a thermally induced glass transition results in a significant loss in chromophore orientation.

Alternatively, an increase in glassy state relaxation rates and a concomitant decrease in the glass transition temperature (T_g) in polymers can be achieved without raising the temperature through the introduction of a diluent into the polymer matrix.[9,10] In our research, chromophores are aligned in an electric field while the matrix is swollen by carbon dioxide. Carbon dioxide is attractive as a diluent for several reasons. First, at elevated pressures CO_2 behaves in a manner characteristic of a polar organic solvent.[11] The polar nature of candidate chromophore−polymer systems dictates the use of polar organic solvents. Second, CO_2 is a very efficient plasticizer. Due to its small size, for a given diluent weight fraction CO_2 lowers T_g further than larger diluent molecules.[12,13] Third, CO_2 has a high solubility when compared with other gases.[11,14] Thus, at ambient temperatures the glass transition pressure (the CO_2 pressure at which the polymer undergoes the glass transition) can be reached at moderate pressures for many candidate polymer materials. Fourth, sorption and desorption of CO_2 in the polymer matrix are easily controlled through the system pressure. Finally, there is no significant residual CO_2 left in the matrix after depressurization to act as a plasticizer. Hence sub-T_g relaxations are minimized and SHG temporal stability improves.

In addition to increasing the alignment of chromophores in polymer systems that have already been studied, CO_2 processing allows the use of polymers which were previously unattractive due to their high T_g's. It has been shown that significant loss of the SHG signal occurs with time due to sub-T_g relaxations of the polymer (although physical aging of the polymer after poling substantially reduces SHG decay).[15,16] Thus to be practical, long-lived NLO systems must be based on highly rigid polymeric matrices which exhibit high T_g values.[17,18] However, the high temperatures needed for

[⊗] Abstract published in *Advance ACS Abstracts,* April 1, 1996.

S0024-9297(96)00235-5 CCC: $12.00

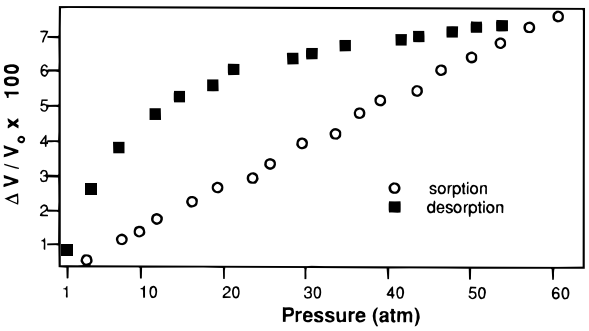

Figure 1. Change in volume of polycarbonate vs CO_2 swelling pressure (data from ref 20).

alignment in some systems can also cause thermal degradation of the chromophore or the polymer or both, so thermally induced glass transitions are precluded. CO_2 processing allows the thermal problems to be circumvented. The number of polymers which can be considered for use as matrix materials is therefore greatly expanded. The novel alignment technique may be applied to poly(ether sulfone)s, polycarbonates, substituted styrenics, acrylates, methacrylates, phenolics, cross-linked epoxy and polyimide systems, and many other high-temperature stable engineering thermoplastics and thermosets.

The use of CO_2 to soften a polymer matrix and allow chromophore rotation also has disadvantages compared to thermal processing. Most importantly, after CO_2 processing the glass may have more free volume, causing faster relaxation of chromophore orientational order. The disruption of glass architecture caused by gas dilation has been observed in gas separation research. Sorption and volumetric behavior of small-molecule penetrants such as N_2, CH_4, and CO_2 in various polymers have been investigated by several groups, notably Paul and Koros and associated researchers at the University of Texas at Austin.[10,19−23] A finding with important implications to our research is that CO_2 swelling (above a certain pressure) of glassy polymers causes an essentially permanent increase in the free volume of a glassy polymer.[14,20] Also, a hysteresis is observed in the CO_2 sorption (and the sample volume) vs pressure data, as evidenced in Figure 1 (data from ref 20). The concentration of CO_2 in the matrix is less in the pressurization half compared to the depressurization half of a swelling cycle. This hysteresis is the result of CO_2 altering the polymer structure.

A fundamental theory describing the hysteresis and the manner in which CO_2 alters the glassy structure has not been forwarded in the literature. Fleming and Koros have hypothesized that "subtle submolecular scale disruptions" in the morphology effectively lower the cohesive energy density of the polymer when it is swollen with CO_2.[14] Note that although the polymer returns close to (but above) the same free volume fraction after conditioning, the structure on small length scales could be substantially different.

The sensitivity of SHG to chromophore orientation relaxation suggests SHG decay as a probe of morphological effects of CO_2 (or other diluent) processing of glassy materials. Previously, we have demonstrated the ability of the CO_2 processing method to align chromophores in host−guest systems with glass transition temperatures up to 180 °C, in a polymer with the chromophore covalently bonded as a side chain, and with the chromophore incorporated in the polymer main chain.[24] Here, CO_2 alteration of glass morphology is explored. The time dependence of the decay at constant temperature and the temperature dependence of the SHG decay after CO_2 processing are examined. The host−guest system of Disperse Red 1 (DR1) in poly(methyl methacrylate) was investigated in much of the work, with polycarbonate also serving as a chromophore host.

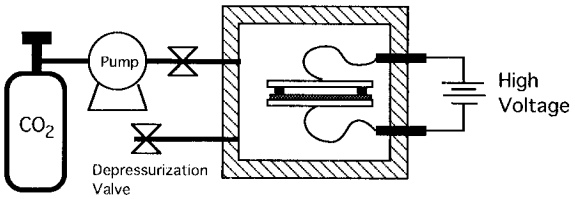

Figure 2. Pressure vessel illustration. The apparatus was used to swell thin polymer films with CO_2. High voltage was applied to the swollen film sandwiched in a parallel-plate capacitor to align the SHG chromophores.

Experimental Method

Film Processing. The polymer−chromophore systems were dissolved in an appropriate solvent and spin cast onto a 150 μm thick glass cover slide. These films ranged in thickness from 0.5 to 1.0 μm. The films were annealed under house vacuum for at least 48 h at elevated temperatures (in the region of the glass transition temperature) prior to poling.

The pressure vessel in which the films were swelled with CO_2 was built by the College of Chemistry Machine Shop at the University of California, Berkeley. The electric field−CO_2 processing setup is illustrated in Figure 2. A Spellman high-voltage dc supply was used to generate the high voltage for chromophore alignment. Kemlon high-voltage electric feedthroughs (Model K-28 BMAHV) allowed the high voltage to be applied to the capacitor. The electric feedthroughs were designed to withstand a maximum of 8000 V dc. The capacitor assembly consisted of the polymer film coated glass cover slide sandwiched between copper disk capacitor plates. Masking tape on the grounded electrode was used as a spacer and allowed CO_2 access to the film surface.

The vessel was filled with CO_2 to a desired pressure. The diffusivity of CO_2 in most glassy polymers ranges from 10^{-9} cm^2/s for an unswelled polymer to 10^{-6} cm^2/s for swelled polymers close to the glass transition composition.[11] Using the unswelled diffusivity, the time constant for CO_2 penetration is approximately 10 s. After pressurization, an electric field in the range of 100 000−500 000 V/cm was applied across the CO_2-swollen film (limited by the maximum voltage that could be supplied through the electric feedthroughs).

After maintaining the pressure at its maximum pressure for a time on the order of minutes, the pressure was reduced at a desired rate, in the range of 0.007−4 atm/min. For selected films, the depressurization was stopped at at low pressure for a period of time. This allowed the feasibility of using low-pressure annealing to decrease the subsequent SHG decay rate to be examined. The depressurization was manually controlled with a Whitey micrometering valve (Model SS 22RS4). The depressurization schedules for the films discussed below are given in ref 25. After complete depressurization, the electric field was turned off, and the film was removed from the pressure vessel for SHG analysis. The time after depressurization until SHG characterization varied. The shortest time between completion of the poling process and SHG measurement was approximately 5 min due to apparatus limitations. Thus the initial decay immediately after turning off the electric field could not be measured.

The effect of dissipation of trapped charges was not accounted for in this work; such charges might affect the observed decay in the first 24 h after poling.[26] The decay seen in Figure 11, taken approximately 15 h after poling, may be particularly affected. Other data were primarily taken at least 24 h after poling, when the injected charge was likely dissipated.

SHG Measurement. An Nd:YAG laser (Spectra Physics DCR 1) with a pulse width of approximately 10 nm and a pulse rate of 10 Hz was used in SHG measurements. The spot size of the unfocused beam had a diameter of approximately 3 mm. The fundamental beam was P-polarized, with an incident angle of 45° relative to the sample. The second harmonic produced by the sample was measured in transmission.

Rapid temperature ramps followed by constant-temperature soaking periods were used to determine the temperature dependence of chromophore relaxation. A ramp and soak temperature program was used to observe SHG decay at various temperatures, yielding information on decay profiles and the temperature dependence of relaxation times. The heating element was a convective air heating gun, controlled by an Omega Model 2010 temperature controller. The sample holder was constructed of copper and allowed rapid heat conduction and stable temperature control.

Due to lack of necessary equipment, in some experiments the sample SHG was measured without a reference. This method yielded acceptable results with minimal power drifts for the ramp and soak measurements experiments performed with the laser kept on and when the lamp power was unchanged. However, when the SHG decay after poling was studied over a period of days and the laser was turned off between measurements, the uncertainty in resetting the laser flashlamp power to the same position was significant. In some experiments a Y-cut quartz SHG reference and the necessary signal processing equipment were available and employed so that the decay of the signal over a period of days could be measured more accurately. The films in which a quartz reference was not used have error bars (determined by the accuracy to which the flashlamp power could be set) shown in Figures 3 and 5.

The SHG light was collected by a Hamamatsu photomultiplier tube, with voltage supplied by a Products For Research high-voltage supply. The signal from the PMT was fed to a Princeton Applied Research Model 164 gated integrator, housed in a Princeton Applied Research Model 162 boxcar averager. The signal from the boxcar averager was collected with a Metrobyte DAS 16 analog to digital board on a personal computer. The sample SHG was compared to the SHG of a quartz reference so that laser power fluctuation and drift would not affect the results. The sample temperature as measured by an Omega J-type thermocouple was converted to millivolts using an Omega TAC 81J thermocouple to analog converter and was also collected with the Metrobyte A/D board. The temperature was measured by the temperature controller was steady and accurate within 1 °C.

The SHG intensity as a function of temperature and time was plotted and the data fit using the software Igor, Version 1.24, by WaveMetrics. Igor also found standard deviations for the fitting parameters.

Results

The results are organized into two sections. First, CO_2 dilation effects are examined. Second, general decay features are delineated and compared to SHG decays in thermally cured systems studied by other researchers.

I. CO_2 Dilation Effects

Here, the influences of both the maximum CO_2 sorption level and the desorption rate on SHG decay are described. Also, chromophore alignment in the glassy state using low CO_2 pressures is presented.

1. Maximum CO_2 Pressure Effect on Polymer Morphology. Figure 3 shows the initial decay at ambient temperatures for two films that were subjected to different maximum pressures. One film was initially swelled with CO_2 at 35 atm (film 1) before being depressurized to 7.8 atm over 8 min. The other film was initially swelled to 7.8 atm (film 2). Both films were annealed at 7.8 atm for 37 h prior to a 4 h depressurization to 1 atm. Film 1 is seen to lose 78% of the SHG in 46 h, as compared to a 40% loss for film 2. Thus, the glass modification from the initial high-pressure swelling was not erased by the 40 h low-pressure annealing. This is similar to the history effect seen by Fleming and Koros.[14] It appears that the decay rate for the two films is similar but that the magnitude of the initial decay for the film exposed to higher CO_2 pressure is greater. The high CO_2 content thus likely introduces more defects in the glass, promoting chromophore motion in their vicinity.

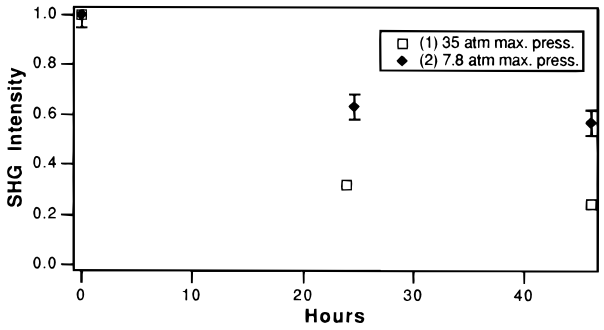

Figure 3. Effect of maximum swelling pressure on initial SHG decay at ambient temperature. Films are PMMA−2% DR1. SHG intensity is normalized by the initial point for each film.

In addition to the experimental error indicated in Figure 3, there are other sources of uncertainty in the loss in intensity. A variation of SHG at different locations on the same film can be seen in our films (this effect is noted by other researchers[15]). Also, approximately 5 min is needed to remove the film from the swelling chamber and position it for SHG characterization. The loss of the signal during this time is not known. Finally, and perhaps most importantly, a small change in the annealing procedure after spin casting can have a large effect on the initial decay. This effect was not examined in our work. The data in Figures 3 and 5 should thus be viewed only as showing the trends in SHG decay characteristics due to the variation of processing conditions.

The effects of the high-pressure swelling are also observable in the temperature step study for each film at 46 h after poling. The signal decreased fairly rapidly at first and then leveled off after roughly 50 h, decaying at a much slower rate (see Figures 11 and 13 for other initial decay studies). This leveling off of the SHG decay (after roughly 50−100 h) was observed for all films studied; the amount of signal remaining after leveling off varied as a function of CO_2 processing conditions, as is discussed below.

We briefly digress here to introduce a general feature of the SHG decay: an apparent bimodal relaxation. A fast decay is followed by a slower decay that appears to be caused by the α-relaxation. Below the glass transition the α-relaxation still occurs, but it follows an Arrhenius temperature dependence.[27] The slow decay's dependence on the α-relaxation is discussed in terms of intermolecular cooperativity in section II.

In this work, we use the KWW equation to fit the SHG decay data at short times. The KWW equation has the form

$$\phi(t) = \phi_0 \exp(-(t/\tau)^b) \qquad (2)$$

where $\phi(t)$ is a measured quantity, here the SHG signal,

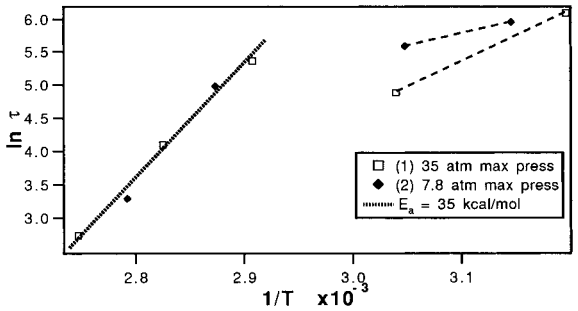

Figure 4. Arrhenius plot of long time decay for PMMA−2% DR1 films swollen to different maximum pressure. Data were taken 46 h after poling. The dashed lines are included to guide the eye.

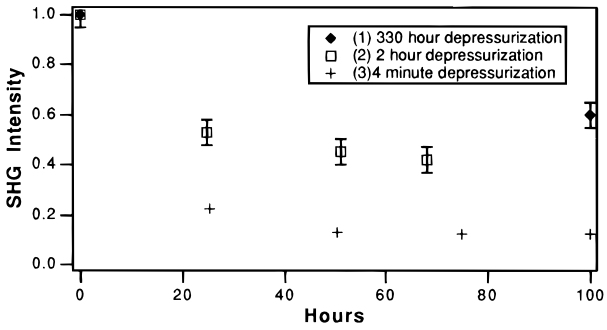

Figure 5. Effect of depressurization rate on initial SHG decay at ambient temperature. SHG intensity is normalized by the initial point for each film.

which decays with time t, ϕ_0 is the value at $t = 0$, τ is the characteristic time constant, and b is termed the stretching exponent, with $0 < b \leq 1$. The KWW equation has been widely employed to describe the relaxations in constrained, disordered media. The KWW equation is used in this work to fit decays that are followed for a relatively short time (roughly 10^3 s).

Returning to Figure 3, at 46 h we expect some chromophore alignment to remain in the fast-relaxing, less dense regions. The Arrhenius plot for the two films in Figure 4 shows that this is the case. The terminal behavior at high temperatures is very similar for both films and displays Arrhenius behavior. Film 1 shows an increase in the time constant with increasing temperature between the second and third low-temperature points. This is likely due to the elimination of chromophore alignment in the fast relaxation zones in the two lower temperature soaks. The more noticeable dip in the film 1 day compared to film 2 is due to a greater percentage of low-density regions in film 1. Thus, if the ambient decay was continued for longer than 46 h, there would have been further fast mode relaxation in film 1.

The terminal decay at high temperatures is seen to closely coincide for the two films, with an activation energy of 35 ± 2 kcal/mol. This activation energy and the time constants are typical of the α-relaxation.[28] If the two low-temperature points for film 1 are assumed to result from a single initial decay mechanism (faster than α), an activation energy of 15 kcal/mol is found. This activation energy is only a rough estimate, with two data points being used. Also, this "initial decay" activation energy is fairly large because it occurs late in the initial decay; the apparent activation energy will likely increase as the initial decay proceeds, due to an increase in constraints.

Our data indicate that films poled at 35 and 7.8 atm have the same terminal Arrhenius dependence. A variety of different processing conditions are also seen to have a negligible effect on the terminal relaxation environment in Figure 8, discussed below. The results thus indicate that the higher pressures alter the glass structure by increasing the percentage of higher mobility regions, while still leaving the dense regions unaffected. This is similar to Fleming and Koros's predictions of an increase in the Langmuir population in the dual-mode model,[20] or an increase in "submolecular disruptions".[14]

2. Effect of Depressurization Rate. The depressurization rate in swelling experiments is expected to have a similar effect on the glassy structure as the cooling rate in thermal experiments. As the rate increases, the glass is frozen further from equilibrium, with a greater amount of free volume trapped in the glass. The slower the depressurization rate, the lower the expected free volume after depressurization is complete. Also, it is likely that with greater initial swelling, the effect of the depressurization rate will be more observable (due to the system being initially displaced further from its final CO_2-free condition).

A series of experiments of PMMA films swelled with CO_2 to 21 atm further demonstrate the importance of the depressurization rate on the initial decay. The final decay of the SHG signal at ambient temperature in three films processed at extremely different depressurization rates is shown in Figure 5; film 1 was depressurized in 333 h, film 2 in 2 h, and film 3 in 240 s. The decays of films 2 and 3 appear to have slowed dramatically after roughly 50 h. As for the slowest depressurized film, the SHG was not measured between the time just after poling and 100 h after poling. It is likely that, as with the other two films, the signal leveled off at roughly 50 h after poling.

Note that the SHG has been normalized for each film independent of the other films; the films do not have the same initial intensity. The difference in intensity cannot be directly attributed to differences in processing conditions using our experimental technique. Such a direct comparison is not meaningful due to differences in thickness between films and to small variations in SHG at different locations on the same film. However, large differences can be easily measured. The "initial value" (taken 6 min after electric field poling) of SHG for film 3 was approximately *4 times less* than for the other two films. If this difference was shown in Figure 5, the SHG at time zero for film 3 would be 0.25. The decay of film 3 before measurement could have taken place during the rapid depressurization of the film while the electric field was on and during the 6 min between turning the electric field off and the start of SHG characterization. In any event, the decay from the maximum signal is actually much greater in film 3 than indicated.

Figure 6 shows an Arrhenius plot of the temperature step studies for each of the films performed after the initial decay appears to be complete. The difference in the decay characteristics is striking. Though the fast depressurized films appeared to be in a plateau region in Figure 5, the decay in these films is clearly proceeding faster than the α-relaxation at lower temperatures. For example, in film 3 the decay at 45 °C is faster than at higher temperatures, suggesting that there is still a high percentage of the aligned chromophores in low-density regions 100 h after poling. At high temperatures, all three films appear to be approaching the same activation energy, as expected. The slow depressuriza-

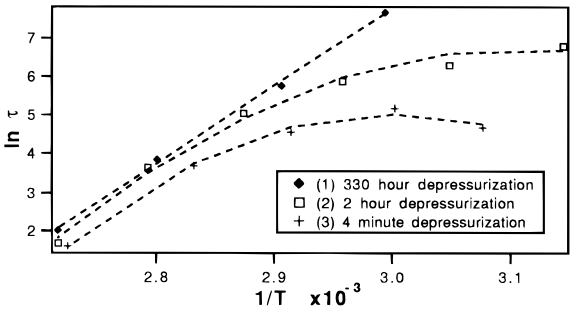

Figure 6. Arrhenius plot of long time decay for PMMA−2% DR1 films depressurized at different rates. The dashed lines are included to guide the eye.

tion yielded a much more stable glass, with the linear behavior in Figure 6 indicating that SHG decay results from only the α-relaxation mechanism.

The decay of film 1 compared to films processed at lower maximum pressures (for example, see film 2 in Figure 4, which was processed at 7.8 atm) demonstrates that slow depressurization (or low-pressure annealing after high-pressure swelling) can reduce the structural disruptions caused by swelling the polymer with higher pressure CO_2.

In terms of Donth's cooperativity concepts,[27] the increase in the initial SHG decay with increasing CO_2 swelling and desorption rate stems from a greater number of α-relaxation precursors and local molecular motions. CO_2 incorporation likely increases the extent of α-precursor relaxations by increasing submolecular disruptions in the cooperative regions. This is discussed in greater detail below.

3. Glassy State Processing. We report here the ability to align the chromophores in the glassy state using CO_2 dilation at reduced pressures. The decay of the SHG signal after alignment is proof of glass-state relaxation mechanisms. However, the relaxation at room temperature in an unswelled state is very slow for higher T_g materials, lasting at least on the order of months (this is very high-T_g materials are desirable for use as SHG films). Diluent swelling at diluent concentrations which are too low to cause a glass transition is a compromise aimed at reducing diluent-induced glass disruptions, while still allowing expedient chromophore orientation. The prediction of alignment times based on T_g reduction through dilation and α-transition relaxation times is discussed in an Appendix.

SHG decay rates for films processed in the glassy state are presented above: PMMA−2% DR1 films swollen to 7.8 and 21 atm and PC−1.5% DR1 films swollen to 21 atm are all in the glassy state (estimated using experimental results from sorption studies of the pure polymers.[10,11,13] Films processed in the glassy state had SHG as large as those processed in the equilibrium material. An example of a film aligned in the glassy state is a PC−DR1 film swelled with CO_2 to 21 atm at ambient temperature for 2 h; this is well below the glass transition pressure (the glass transition is still not reached at 61 atm for pure PC[11,14]). The initial SHG signal from this film was as strong as that produced by a film swollen beyond the glass transition, indicating that chromophore alignment was attained in the dense regions of the glass. Films that had smaller initial SHG signals were PMMA films processed at 7.8 atm for 15 min; the signals for these films were approximately 40% smaller than a completely aligned sample.

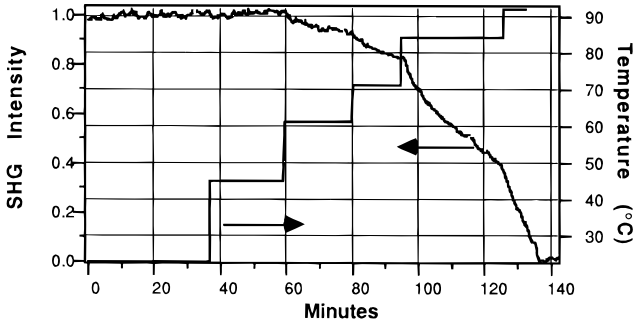

Figure 7. SHG decay in the PMMA−DR1 system. Film is 2 wt % DR1, swollen to 21.4 atm with CO_2; 334 h poling and depressurization time. Data were taken 100 h after poling. The decay of SHG was observed sequentially at 23, 45, 61, 71, 84, and 92 °C.

Table 1. KWW Parameters for Decays Shown in Figure 7

temp (°C)	τ (min)	std dev	b	std dev
61	2082	414	0.54	0.02
71	311	30	0.77	0.02
84	48	0.5	0.88	0.01
92	7.5	0.1	1.0	0.1

II. General Decay Characteristics

As discussed in the previous section, a multimodal decay is indicated in our results. A fast initial SHG lasting approximately 50−100 h was observed for all films studied; the amount of signal remaining after leveling off of initial decay varied as a function of CO_2 processing conditions. The initial decay is given a cursory examination in this work, following a more detailed analysis of the slow final decay in the following section.

1. Terminal Arrhenius Behavior. After the initial decay is completed, the relaxations are observed in sequential temperature step studies to approach Arrhenius behavior, using the KWW equation to fit the data. Figure 7 shows the relaxation 100 h after poling for a PMMA−DR1 film. The decays at 23 and 45 °C 100 h after poling were too slow to be observed in the time frame of the experiment. The decays after the four higher temperatures were fit using a KWW expression. Table 1 summarizes the results. The stretching exponent b is seen to increase from 0.54 to 61 °C to 1.0 at 92 °C. The increase in b toward unity near the glass transition as shown in Table 1 is commonly observed in our results.[20] In terms of a distribution of environments, the increase in b can be interpreted as the approach to one relaxation environment. Because the temperature steps are done sequentially, this approach to a single relaxation environment might be expected as an artifact of the experimental procedure (see the discussion of the KWW equation below and the memory effect in the Appendix). However, Walsh et al.[17] have seen similar behavior in individual decay experiments carried out at different temperatures.

The time constants given in Table 1 are plotted in Figure 8, along with those from several other PMMA−DR1 films. The films are examined at a range of times after poling, as indicated in the legend of Figure 8. The poling pressure and poling time for each film are given in Table 2.

The five films shown in Figure 8 were characterized after most of the initial decay is complete and generally follow Arrhenius behavior. A fit of the data from films 2, 3, and 4 in the "terminal" (asymptotic) linear region yields an activation energy of 37 ± 3 kcal/mol (this is

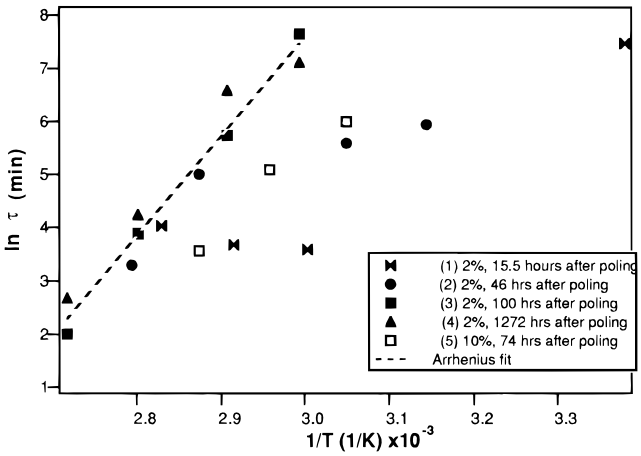

Figure 8. PMMA−DR1 time constant temperature dependence. The dye weight percent and the time that the SHG was observed after poling for each film are indicated in the legend. The Arrhenius fit is for the two high-temperature points of (1) and all points of (2) and (3).

Table 2. Electric Field Poling Time and Maximum CO_2 Pressure

	film				
	a	b	c	d	e
poling time (h)	343	41.5	333	22.3	15.7
max CO_2 (atm)	35	7.8	21.4	21.4	14.6

within the standard deviation of the 35 kcal/mol found for the three films in Figure 4). This activation energy and the time constants are typical of the α-relaxation.[28] In materials above T_g, the α-relaxation is observable as the loss peak in dielectric and dynamic mechanical spectroscopy and through the increase in time scale (viscosity) as the temperature approaches the glass transition from above.[9,29] The faster-than-Arrhenius increase (increasing apparent activation energy with decreasing temperature) of the α-relaxation time constant above T_g is well described by the Williams−Landel−Ferry (WLF) equation.[30] Below the glass transition, the α-relaxation still occurs, but it follows an Arrhenius temperature dependence.[27] This change in temperature dependence is a result of the "freezing-in" of the relaxing structure at T_g; the material is not in thermodynamic equilibrium on an experimental time scale. The nonequilibrium structure of glassy polymers is discussed in terms of intermolecular cooperativity below.

At higher temperatures, the decay in film 1 of Figure 8 observed 41 h after poling approaches the same slope observed for the films where SHG decay was measured long after poling. This is in accord with the notion that once the initial decay is complete, there is a single relaxation mechanism. Film 5, containing 10% DR1, is included in Figure 8 to demonstrate that the activation energy is relatively independent of the dye concentration. Note that the relaxation times for film 5 are shifted to lower values at a given temperature compared to the 2% dye films, due to the decrease in T_g with an increase in dye concentration (a plasticization effect). The correlation of the relaxation time constant with diluent concentration and T_g has also recently been noted by Dhinojwala and Torkelson.[31]

The results of other researchers of host−guest SHG systems also indicate a SHG decay dependence on the α-relaxation mechanism. Dhinojwala and Torkelson explicitly noted the α-relaxation dependence seen in

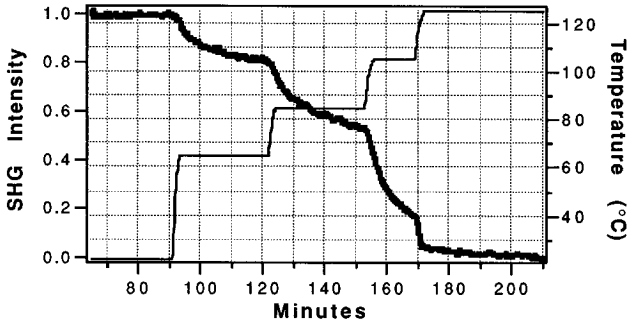

Figure 9. SHG decay in the PC−DR1 system. The film is 1.5 wt % DR1, swollen with CO_2 at 21 atm; 56 h poling and depressurization time. Data were taken 38.3 h after poling. The temperature was stepped from ambient to 65, 85, 105, and 125 °C.

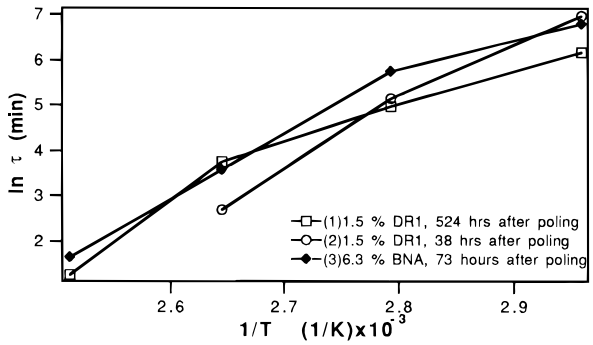

Figure 10. Arrhenius plot for PC films. A fit of film 2 yields an activation energy of 27 kcal/mol. Note the slight curvature of the data for all of the films. The lines between data points are drawn to guide the eye only.

their results.[31] Walsh et al. found that one universal equation (similar to the Vogel−Fulcher−Tammann (VFT) equation[32,33] but with weaker-than-Arrhenius temperature dependence) was able to fit the temperature dependence of the KWW time constant for many different film types studied.[17] Walsh notes that the chromophores had to be "large" for the use of a single fitting equation. Smaller chromophores were found by Walsh to relax much faster than the larger chromophores, indicating that they could relax independently of the α-relaxation. While the source of the non-Arrhenius functionality is not clear, the existence of a temperature-dependent relaxation that is independent of the host−guest system suggests that the α-relaxation controls the SHG decay and has a length scale that is much greater than the chromophore size.

Arrhenius Decay in PC Films. Arrhenius behavior is also seen in PC films. Figure 9 shows the temperature program and the decay of SHG intensity for a PC film taken 38 h after poling. An Arrhenius plot of the time constants from this decay as well as for two other films is shown in Figure 10. The data from Figure 10 yield an activation energy of 27 kcal/mol. This is somewhat smaller than the activation energies observed for the PMMA films. The chromophore BNA (4-(dimethylamino)-4′-(dimesitylboryl)azobenzene, a large boron-containing chromophore that has two aromatic groups attached to the electron-accepting boron group (synthesized by M. Lequan and co-workers at ESPCI)) is also used here, providing similar results to DR1 films. Note the slight non-Arrhenius temperature behavior indicated in all of the PC decays, even in the film examined long after (524 h) poling. This may be an indication that faster-than-α relaxations are still occur-

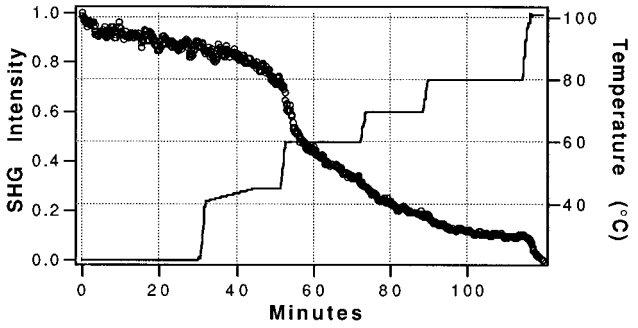

Figure 11. PMMA−DR1 system. Film is 2 wt % DR1, swollen at 35 atm with CO_2; 343 h poling and depressurization time. Data were taken 15.25 h after poling. The fluctuations in the temperature reading are artifacts of the data collection.

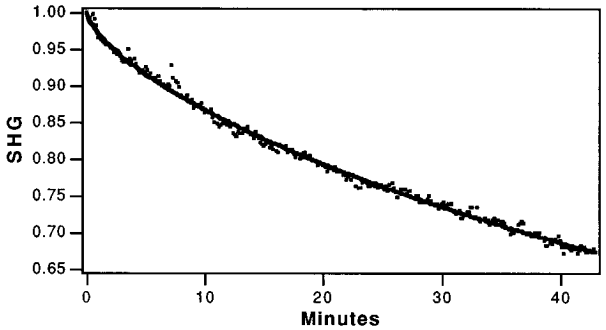

Figure 12. Initial decay at 65 °C after a temperature step from 55 °C in a PMMA−10% DR1 film, fit by the KWW equation: $\tau = 163$ min, $b = 0.70$. This time constant and the time constant at 55 and 75 °C are shown in Figure 8, film d.

ring in the PC samples studied. However, the same non-Arrhenius behavior was also observed by Walsh.[17]

Cooperativity and the α-Transition. The apparent dependence of the long time relaxation on the α-relaxation mechanism can be addressed through cooperativity concepts. Cooperativity was first proposed by Adams and Gibbs to explain the precipitous decrease in the α-relaxation rate as a material is cooled toward the glass transition temperature.[34] All cooperativity models share a basic theme, as follows. In dense liquids near the glass transition, the motion of molecules (or molecular segments) depends on cooperative movements of surrounding molecules. Lengthening of the α-relaxation time scale (increasing degree of cooperative motion) is universally observed in materials approaching the glass transition from a high temperature, and is indicated by WLF scaling. At the glass transition, the growth of cooperative regions is halted. Arrhenius behavior is then observed for the α-relaxation below T_g.

Our results indicate that the slow decay of chromophore orientation is caused by the α-relaxation. Using thermodynamic fluctuation theory to describe cooperativity, Donth calculates that the size of the cooperative regions at the glass transition in polymers involves on the order of 100 molecular segments, leading to a characteristic length scale of 1−4 nm for the α-relaxation.[27,35] This length scale is large compared to the size of a chromophore. Thus, the slow SHG decay below T_g is likely caused by the relaxation of the glassy structure surrounding a chromophore molecule.

2. Initial Fast Decay. For the films where SHG decay is observed shortly after poling in Figure 8, the decrease in relaxation times with increasing temperature does not follow Arrhenius behavior. This is interpreted as evidence of a distribution of relaxation environments, with chromophore alignment in the fast-relaxing regions being lost at lower temperatures. As the temperature is increased, the decay is observed for chromophores in more highly constrained regions, so an Arrhenius-like decrease in the time constant with increasing temperature is not observed. The fast relaxing regions are still active, but in them there is no correlation of chromophore orientation.

The loss of chromophore alignment in the less dense regions of the glass can also be seen in Figure 11 (the time constants for the decays in this figure are given as film 5 in Figure 8). Again, rather than waiting 24 h or more before performing a temperature ramp−soak study, the film was heated after 15 h. As can be seen, there is a very large decrease in SHG signal at about 55 °C. The signal does not decrease as rapidly after this drop at higher temperatures.

The rapid decrease followed by the plateau indicates at least a binary environment. The sharp decay at the 40−60 °C temperature ramp indicates the loss of chromophore alignment in low-density regions. It is unlikely that this decay is the result of CO_2 exiting the film, since the experiment is carried out 15 h after depressurization and removal of the CO_2 atmosphere. A relatively high activation energy is indicated in this initial decay region by the relatively steep slope. Also, the sharp decay here reveals a problem with the sequential ramp and soak method. The large decrease in signal occurs mainly during the temperature ramp; hence it is not included in the KWW fits at either 45 or 60 °C. If the ramp could be done faster, this rapid decay could be included in a KWW fit, and it would have a much faster time constant/lower b.

Cooperativity concepts, introduced above in discussion of the α-relaxation and Arrhenius decay, can also qualitatively suggest mechanisms for fast initial SHG decays. Donth defines the structure of a cooperating region as containing one free volume hole.[27] In the immediate vicinity of the hole, molecular segments may relax independently and faster than the α-relaxation. In addition to the "hole", there are subhole packing disruptions that may lead to α-precursor molecular motions, such as Andrade modes.[36,37] Local chromophore motion near a defect, a β-transition, Andrade modes, and the fast-relaxing shoulder of the main transition spectrum could all contribute to the initial decay observed after the poling field is turned off, and perhaps to the initial decay after a temperature step.

3. Multimodal Distribution and the KWW Equation. The KWW expression provided a good fit of decays at short times (in the range of 1 h) after temperature steps. For instance, Figure 12 shows a typical decay after a temperature step from 55 to 65 °C for a PMMA−DR1 film. For many other glassy state experiments (e.g., dielectric, creep, Kerr effect, etc.; Ngai provides an extensive review[38]), a KWW decay over the entire relaxation is observed. Other researchers have examined the ability of the KWW equation to describe an entire SHG decay, yielding varying degrees of success. In one recent study, the SHG decay was reported to be well fit by the KWW equation over 11 decades in time.[31] In other studies (discussed below) the KWW fit was less accurate, due to an apparent bimodal decay.

It has been speculated by some researchers that the KWW form results from a distribution of relaxation times.[31] From the distribution viewpoint, as the width of the distribution increases, the stretching exponent of the KWW equation decreases from unity. These researchers believe that a distribution of relaxation time

constants is the source of the stretched exponential behavior. However, the KWW equation cannot approximate all distributions. For distributions such as a bimodal decay, the KWW equation is inadequate; the KWW equation predicts $\phi(t=\tau)/\phi_0 = 1/e$ regardless of the value of b. This is the primary reason the KWW has difficulty in fitting some SHG decay. The biexponential form seen in eq 3 has no such constraint, due to the preexponential weighing constants

$$\phi(t) = \phi_f \exp(-t/\tau_f) + \phi_s \exp(-t/\tau_s) \qquad (3)$$

where the subscripts f and s indicate the fast and slow decay parameters, respectively, ϕ_f and ϕ_s are weighting constants such that $\phi_f + \phi_s = 1$, and τ_f and τ_s are time constants.

Equation 3 does not fit our data well after temperature steps. But Lindsay et al., using thermal processing for chromophore alignment, found the biexponential decay to fit his SHG decay data much better than the KWW equation.[39] Lindsay examined the relaxation after thermal processing of a chromophore side chain at different temperatures. A fast initial decay was followed by a much slower decay, both being well fit by a single exponential. The sharp change in the relaxation produced by the large difference in the two time constants was much more distinct than that observed in our experiments or in the data of other researchers. This may be due in part of the attachment of the chromophore as a side chain, with the covalent bond disallowing translational diffusion of the chromophore, and constraining it from changing environments. Additionally, though not as conclusive as Lindsay's data, the data of Walsh et al. also bring into question the appropriateness of the KWW equation in fitting an entire decay.[17] The KWW equation was used to fit the decay of several different types of polymer−chromophore films, but Walsh noted that a biexponential fit the decay as well as the KWW equation. The KWW fit is therefore likely only approximate.

Returning our discussion to the physical origins of the KWW expression, we note that other derivations contend that a distribution of relaxation environments is not the source of stretched exponential behavior. Instead, KWW relaxation is thought to result from some fundamental physics in dense, constrained media.[40−42] For example, Ngai has forwarded the "coupling model" theory, in which identically relaxing species, which exhibit pure exponential relaxation at very short times, diffuse in a KWW fashion due to correlated motion with each other.

However, Ngai has found cases where a single KWW expression, and thus a single relaxing environment, was insufficient in describing a decay. For local relaxations in polycarbonate, Ngai resorted to a distribution of KWW relaxation environments.[43] Citing similar complex cases such as this, Ngai has speculated that the overall relaxation function is the result of a distribution of contributions from various homogeneous relaxing species (which themselves exhibit KWW decay).[44] Thus, a fast decay for chromophores residing in relatively unconstrained microenvironments would occur in parallel with a slow decay that proceeds via a different mechanism for chromophores residing in denser, more constrained microenvironments.

A combination of the concepts of a distribution of KWW relaxations and a bimodal decay, such as eq 4, could be considered:

$$\phi(t) = \phi_f \exp(-(t/\tau_f)^{b_f}) + \phi_s \exp(-(t/\tau_s)^{b_s}) \qquad (4)$$

A dual KWW expression, with stretching exponentials b_f and b_s for the slow and the fast relaxations, would provide a great deal of flexibility in fitting SHG relaxation. Wang et al. have recently considered the same function in describing SHG relaxation in a corona poled, thermally processed film.[45] Equation 4 breaks the decay into two gross time scales τ_f and τ_s. Within each of these regions KWW relaxations indicate either finer distribution of relaxation environments or a single relaxation mechanism, i.e., Ngai's coupling model. Due to the disruption of portions of the polymer structure by CO_2 swelling, an expression such as eq 4 is likely to be needed to fit the entire SHG decay for CO_2-processed polymer films.

Conclusions

In the host−guest systems studied, a fast initial decay of SHG is followed by a slower decay that appears to be determined by the α-relaxation. Cooperativity can explain to a large extent the slow decay by invoking the α-relaxation. However, the initial decay is only addressed qualitatively in our cooperativity discussion. The initial fast decay before the α-relaxation behavior is a function of CO_2 processing conditions. The maximum CO_2 pressure and the depressurization rate both have a dramatic influence on SHG signal stability. The fast initial decay (before the slow α-relaxation) increased as the maximum CO_2 pressure was increased and as the desorption rate increased. Thus, both low-pressure alignment and slow depressurization should be employed to attain the most stable SHG signal. The time constant and temperature dependence of the slow decay was unaffected by CO_2 processing. The results thus indicate that the higher pressures alter the glass structure by increasing the percentage of higher mobility regions while still leaving the dense regions unaffected.

Chromophore alignment was achieved in the glassy state when the glass was swelled with CO_2 at a pressure that was too low to cause the glass transition. This is expected to be important for the SHG processing of high-T_g polymers such as polyimides and epoxies where it is difficult to swell the material through the glass transition.

Future research possibilities include an *in situ* decay study of a CO_2-swollen polymer film. Such a study would provide valuable information on the manner in which CO_2 alters the glassy structure. Also, CO_2 processing of high-T_g systems, including cross-linked matrices, would be insightful.

Appendix: Predicting Alignment Time vs Pressure

The increase in chromophore alignment rate in the glassy state with diluent sorption can be modeled by considering the increase in the α-relaxation rate with diluent sorption. Our SHG results suggest the rotation of chromophores is strongly coupled to the α-relaxation process. We assume an Arrhenius temperature dependence for the α-relaxation and that the increase in the α-relaxation rate is solely due to the increase in T_g with swelling. The lowering of the glass transition temperature for PMMA−DR1 was estimated from data for pure PMMA.[13] The decrease in the glass transition temperature for PC−DR1 was estimated using a relation derived by Chow.[12] Due to lack of experimental data

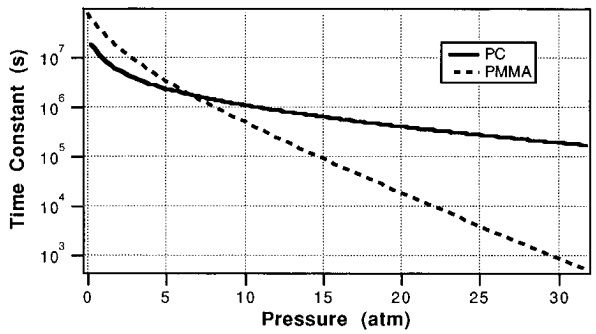

Figure 13. Predicted decrease of the relaxation time constant with diluent sorption in PMMA and PC, based on the lowering of the glass transition, and α-relaxation time constant.

or theoretical predictions, we also assumed that the activation energy of the α-relaxation is independent of CO_2 concentration. Thus, activation energies determined from the SHG decay results presented in this work were employed.

By comparing the curve in Figure 13 to our experimental result that chromophore alignment is possible in PC at 21 atm in less than 7×10^3 s, T_g reduction is seen to underpredict the chromophore relaxation in PC (note that we only know that the alignment was completed by this time; alignment may have been completed more quickly). Actually, the alignment time constant may be smaller than the decay time constant, as was observed in Kerr effect experiments performed on glassy PMMA by Jungnickel.[46] Lacking information, we assume the alignment and decay time constant are equivalent.

The underprediction of relaxation times seen in Figure 13 indicates that CO_2 incorporation induces additional alterations in the glass beyond lowering the glass transition temperature. For example, it is likely that the α-relaxation activation energy is lowered in the swollen film. However, quantitative prediction of this effect is not apparent. Alternatively, CO_2 sorption may decouple the chromophore relaxation from the α-relaxation. For instance, the congregation of CO_2 molecules in the vicinity of chromophore molecules (nanoheterogeneity) would result in such a decoupling. There may be different mechanisms for alignment in the swelled material compared to decay in an unswelled material. In swelled films, CO_2 may cause fluctuations in the glass environment that allow chromophore rotation via large-angle steps, independent of the α-relaxation (alignment in this case is predicted by a fluctuation diffusion model[46]). Finally, the concepts of fragility[47] and cooperativity[27] may provide insight into the alteration of glassy structure through CO_2 addition. Note that an information experiment would be an *in situ* SHG study of chromophore alignment in the swollen polymer.

References and Notes

(1) Prasad, P. N.; Williams, D. J. *Introduction to Nonlinear Optical Effects in Molecules and Polymers*; John Wiley and Sons, Inc.: New York, 1991.
(2) Williams, D. J. *Nonlinear Optical Properties of Organic and Polymeric Materials*; American Chemical Society: Washington, DC, 1983.
(3) Cross, G. H.; Donaldson, A.; Gymer, R. W.; Mann, S.; Parsons, N. J.; Haas, D. R.; Man, H. T.; Yoon, H. N. *Proc. SPIE* **1989**, *79*, 1177.
(4) Stegeman, G. I.; Seaton, C. T.; Zanoni, R. Workshop on the Molecular Engineering of Ultrathin Polymeric Films, Davis, CA, 1987, p 231.
(5) Shen, Y. R. *The Principles of Nonlinear Optics*; Wiley: New York, 1984.
(6) Singer, K. D.; Sohn, J. E.; Lalama, S. J. *Appl. Phys. Lett.* **1986**, *49*, 248.
(7) Meredith, G. R.; Dusen, J. G. V.; Williams, D. J. In *Nonlinear Properties of Organic and Polymeric Materials*; Williams, D. J., Ed.; ACS Symposium Series 223; American Chemical Society: Washington, DC, 1983.
(8) Kielich, S. *IEEE J. Quantum Electron.* **1969**, *5*, 562.
(9) Ferry, J. D. *Viscoelastic Properties of Polymers*; Wiley: New York, 1980.
(10) Chiou, J. S.; Barlow, J. W.; Paul, D. R. *J. Appl. Polym. Sci.* **1985**, *30*, 2633.
(11) Berens, A. R. AICHE Annual Meeting, New York City, 1987, Paper 37e.
(12) Chow, T. S. *Macromolecules* **1980**, *13*, 362.
(13) Wissinger, R. G. Thermodynamic Behavior of Glassy−Polymer/CO_2 Systems at Elevated Pressures, Ph.D., Thesis, University of Delaware, 1988.
(14) Fleming, G. K.; Koros, W. J. *Macromolecules* **1990**, *23*, 1353.
(15) Hampsch, H. L.; Yang, J.; Wong, G. K.; Torkelson, J. M. *Polym. Commun.* **1989**, *30*, 40.
(16) Meredith, G. R.; Dusen, J. G. V.; Williams, D. J. *Macromolecules* **1982**, *15*, 1385.
(17) Walsh, C. A.; Burland, D. M.; Lee, V. Y.; Miller, R. D.; Smith, B. A.; Twieg, R. J.; Volksen, W. *Macromolecules* **1993**, *26*, 3720.
(18) Ye, C.; Marks, T. J.; Yang, Y.; Wong, G. K. *Macromolecules* **1988**, *21*, 2899.
(19) Paul, D. R.; Koros, W. J. *J. Polym. Sci., Polym. Phys. Ed.* **1976**, *14*, 676.
(20) Fleming, G. K.; Koros, W. J. *Macromolecules* **1986**, *19*, 2285.
(21) Chan, A. H.; Paul, D. R. *Polym. Eng. Sci.* **1980**, *20*, 87.
(22) Jordan, S. M.; Koros, W. J. *J. Membr. Sci.* **1990**, *51*, 233.
(23) Barbari, T. A.; Koros, W. J.; Paul, D. R. *J. Polym. Sci., Polym. Phys. Ed.* **1988**, *26*, 729.
(24) Barry, S. E.; Soane, D. S. Materials Research Society Spring Meeting, San Francisco, 1992, 277.
(25) Barry, S. E. Carbon Dioxide Processing of Thin Polymer Films for Second Order Nonlinear Optical Applications, Ph.D. Dissertation, University of California at Berkeley, 1994.
(26) Mortazavi, M. A.; Knoesen, A.; Kowel, S. T.; Higgens, B. G.; Dienes, A. *J. Opt. Soc. Am. B* **1989**, *6*, 733.
(27) Donth, E. J. *Relaxation and Thermodynamics in Polymers*; Akademie Verlag: Berlin, 1992.
(28) Matsuoka, S. *Relaxation Phenomena in Polymers*; Carl Hanser Verlag: New York, 1992.
(29) Hedvig, P. *Dielectric Spectroscopy of Polymers*; John Wiley & Sons: New York, 1977.
(30) Williams, M. L.; Landel, R. F.; Ferry, J. D. *J. Am. Chem. Soc.* **1955**, *77*, 3701.
(31) Dhinojwala, A.; Hooker, J. C.; Torkelson, J. M. *J. Non-Cryst. Solids* **1994**, *172*, 286.
(32) Vogel, H. *Phys. Z.* **1921**, *22*, 645.
(33) Tammann, G.; Hesse, G. *Z. Anorg. Allg. Chem.* **1926**, *156*, 245.
(34) Adam, G. A.; Gibbs, J. H. *J. Chem. Phys.* **1965**, *43*, 139.
(35) Donth, E. J. *J. Non-Cryst. Solids* **1982**, *53*, 325.
(36) Andrade, E. N. d. C. *Proc. R. Soc. London* **1910**, *A84*, 1.
(37) Plazek, D. J. *J. Non-Cryst. Solids* **1991**, *131*, 836.
(38) Ngai, K. L. In *Non-Debye Relaxation in Condensed Matter*; Ramakrishnan, T. V., Raj Lakshmi, M., Eds.; World Scientific: Singapore, 1987; p 23.
(39) Lindsay, G. A.; Henry, R. A.; Hoover, J. M.; Knoesen, A.; Mortazavi, M. A. *Macromolecules* **1992**, *25*, 4888.
(40) Ngai, K. L.; Mashimo, S.; Fytas, G. *Macromolecules* **1988**, *21*, 3030.
(41) Palmer, R. G.; Stein, D. L.; Abrahams, E.; Anderson, P. W. *Phys. Rev. Lett.* **1984**, *53*, 958.
(42) Blumen, A. In *Molecular Dynamics and Relaxation Phenomena in Glasses*; Dorfmuller, T., Williams, G., Eds.; Lecture Notes in Physics 277; Springer-Verlag: Berlin, 1987; pp 1−15.
(43) Ngai, K. L.; Rendell, R. W.; Yee, A. F. *Macromolecules* **1988**, *21*, 3396.
(44) Nelson, K.; Spiess, H.; Montrose, C. J.; Rossler, E. *J. Non-Cryst. Solids* **1991**, *131*, 378.
(45) Wang, H.; Jarnagin, R. C.; Samulski, E. C. *Macromolecules* **1994**, *27*, 4705.
(46) Jungnickel, B. J. *Polymer* **1981**, *22*, 720.
(47) Angell, C. A. *J. Non-Cryst. Solids* **1991**, *131*, 13.

MA960235O